ern boundary current during the last glacial maximum, but its SST's were lower than those today and its transport may have been less. The anomaly patterns also imply that more of the Agulhas is entrained in the West Wind Drift during February than in August.

Third, maps of ΔSST_z at 18,000 years B.P. (Fig. 2, C and D) show that equatorward flow (negative ΔSST_z's) around the subtropical gyre occurred as a distinct eastern boundary current along Australia, whereas today the return flow is concentrated offshore between 90° and 105°E. This observation is consistent with the suggestion of Prell *et al.* (*10*) that since the Subtropical Convergence was located at about 35°S at 18,000 years B.P., easterly flowing water (associated with the West Wind Drift) would be deflected equatorward along the coast of Australia. This northward advection would produce the negative ΔSST_z's along the coast. Webster and Streten (*11*) have come to a similar conclusion based on the more equatorward position of sea ice and the westerlies during the last glacial maximum.

Finally, large negative ΔSST_z's did not occur in the northwestern Indian Ocean during August at 18,000 years B.P. (Fig. 2D). The lack of these negative anomalies indicates less upwelling then than today. Decreased upwelling, in turn, implies that the southwest monsoon was weaker then. During this interval, the Somali Current was also weak and may even have flowed southward. These results are supported by faunal indicators of upwelling (*7, 12*) and by several general circulation model simulations of the ice-age atmosphere (*13, 14*). Furthermore, because monsoon intensity is influenced more by increased continental albedo than by reduced SST (*14*), this anomaly pattern confirms the simulation of the weak ice-age monsoon by Manabe and Hahn (*14*).

Maps of zonal anomalies of SST can be used to identify circulation patterns in modern oceans and their ancient counterparts. Although the mapping technique is highly informative, it requires quantitative estimates of SST on a synchronous basis and accurate plotting of isotherms. Properly drawn, the ΔSST_z map reflects the thermal contrast across an ocean basin and thus the dominant circulation patterns.

WARREN L. PRELL
CLIMAP, *Department of Geological Sciences, Brown University, Providence, Rhode Island 02912*
WILLIAM H. HUTSON
CLIMAP, *School of Oceanography, Oregon State University, Corvallis 97331*

References and Notes

1. G. Neumann and W. J. Pierson, Jr., *Principles of Physical Oceanography* (Prentice-Hall, Englewood Cliffs, N.J., 1966).
2. R. G. Barry and R. J. Chorley, *Atmosphere, Weather, and Climate* (Holt, Rinehart & Winston, New York, 1970).
3. A. Defant, *Physical Oceanography* (Pergamon, New York, 1961), vol. 1, p. 645.
4. CLIMAP Project Members, *Science* **191**, 1131 (1976).
5. R. M. Cline and J. D. Hays, Eds., *Geol. Soc. Am. Mem.* **145** (1976).
6. August and February SST data for the modern ocean were digitized on a grid with 2° by 2° spacing by D. Hahn of the Geophysical Fluid Dynamics Program, Princeton University. The data sources are *World Atlas of Sea Surface Temperatures* (Publ. 225, U.S. Navy Hydrographic Office, Washington, D.C., ed. 2, 1944), and *Monthly Charts of Mean, Minimum and Maximum Sea Surface Temperature of the Indian Ocean* (Spec. Publ. 99, U.S. Navy Oceanographic Office, Washington, D.C., 1967).
7. W. L. Prell, W. H. Hutson, D. F. Williams, A. W. H. Bé, in preparation. Sea-surface temperature estimates for February and August conditions at 18,000 years B.P. are based on planktonic foraminiferal transfer function FI-2, which is discussed in W. H. Hutson and W. L. Prell (*J. Paleontol.*, in press).
8. J. D. Hays, personal communication.
9. K. Wyrtki, in *Ecological Studies, Analysis and Synthesis*, B. Zeitzschel, Ed. (Springer-Verlag, New York, 1973), vol. 3; *U.S. Navy Marine Climatic Atlas of the World*, vol. 3, *Indian Ocean* (Government Printing Office, Washington, D.C., 1976).
10. W. L. Prell, W. H. Hutson, D. F. Williams, *Mar. Micropaleontol.*, in press.
11. P. J. Webster and N. A. Streten, *Quat. Res. N.Y.* **10**, 279 (1978).
12. W. L. Prell, in *Evolution of Planetary Atmospheres and Climatology of the Earth* (Centre National d'Etudes Spatiales, Nice, France, 1979), p. 149.
13. W. L. Gates, *Science* **191**, 1138 (1976).
14. S. Manabe and D. G. Hahn, *J. Geophys. Res.* **82**, 3889 (1977).
15. We thank J. Imbrie, T. Webb, and A. McIntyre for their comments on the manuscript. Supported by NSF grant OCE77-22888 to W.L.P. and NSF grant OCE77-23162 to W.H.H.

9 May 1979; revised 6 July 1979

BK Virus DNA: Complete Nucleotide Sequence of a Human Tumor Virus

Abstract. *The complete DNA sequence of the human papovavirus BK is presented. From the 4963 base-pair sequence of BK virus (MM strain), the amino acid sequence of at least five proteins can be deduced: a T antigen and a t antigen, which share amino terminal peptides; proteins VP2 and VP3, which share 232 amino acids; and protein VP1, whose coding sequence overlaps those for VP2 and VP3 by 113 nucleotides but is read in a different frame. The gene loci and the arrangement of genes are strikingly similar in BK virus and simian virus 40 (SV40). The sequence of the deduced proteins in BK virus shares 73 percent amino acid homology with those in SV40, whereas the DNA sequence of the two viruses shares 70 percent homology, suggesting close evolutionary relationship. However, the repeated DNA sequences in the noncoding regions of these viruses are different.*

BK virus (BKV) is a virus of human origin discovered by Gardner *et al.* (*1*). A variant of BKV, termed the MM strain, was later isolated (*2*) from the brain tumor and the urine of a patient with Wiskott-Aldrich syndrome, a genetic disorder characterized by defects of the immune system. This disease has been associated with a high incidence of malignancies of the reticuloendothelial system (*3*). The evidence for the human origin of BKV and BKV(MM) includes their isolation from humans, the preferential growth of the virus in human cells (*4, 5*), and the presence of BKV-specific antibodies in 70 percent of the adult population (*6-8*). The genome of BKV is a closed circular duplex DNA molecule of 3.45×10^6 daltons, whereas that of BKV(MM) is 3.26×10^6 daltons (*9*). Howley *et al.* showed, by hybridization analysis and physical mapping (*9*), that BKV (prototype or wild type) and BKV(MM) are essentially identical. We have constructed more detailed physical maps of the genomes of wild-type BKV(WT) and BKV(MM) and have found differences only between map positions 0.52 and 0.71 (*10*).

Both BKV and SV40 are primate papovaviruses. Each genome consists of only 5200 base pairs. The simplicity of the viral genome and the limited coding capacity require that they depend on host enzymes for replication, transcription, and translation. Because of the close relation with their host cells, these viruses are useful models for understanding gene action and the regulation of transcription and translation in more complex eukaryotic cells.

In human fetal cells BKV reproduces lytically. It can also transform normal hamster cells in vitro as well as produce tumors in vivo when injected into hamsters (*7, 11, 12*). One consequence of productive infection of human cells by BKV is the induction of nuclear tumor antigen (T antigen) that reacts with serum from animals bearing BKV-induced tumors (*7*). The T antigen has been implicated as an important factor in the initiation of viral DNA synthesis and in the induction and maintenance of transformation (*13, 14*). Tumor antigens induced in virus-infected cells or transformed cells by BKV or SV40 are similar, since each reacts strongly with the

0036-8075/79/1026-0456$00.50/0

heterologous antiserum (*7, 8, 12*). Physical studies confirm this antigenic relatedness. On the basis of coelution by ion-exchange chromatography, seven pairs out of 21 BKV and 20 SV40 tryptic polypeptides are shown to be similar (*15*).

At least three structural proteins from BKV have been identified (*4, 16*). Virus protein 1 (VP1) of BKV is slightly smaller than that of SV40, whereas VP2 and VP3 are similar in size to the corresponding proteins of SV40.

The extent of DNA sequence homology between the genomes of BKV and SV40 varies according to the hybridization technique used. Under stringent hybridization conditions, an overall homology of 11 to 20 percent between the viruses has been reported (*9, 17*). Up to 50 percent homology was obtained when less stringent hybridization conditions were used (*18*). Electron microscopic visualization of heteroduplexes formed at different effective temperatures indicated approximately an 85 percent sequence homology between the genomes of these two viruses (*19*). A recently improved filter hybridization technique also shows extensive homology between BKV and SV40 (*20*). Dhar *et al.* determined the DNA sequence of BKV near the origin of DNA replication (*21*) and found extensive similarity between BKV and SV40, especially in the secondary structures. Reports on portions of the DNA sequence of BKV(WT) (*21, 22*) and BKV(MM) have appeared (*10, 23, 24*). We have determined the complete DNA sequence of BKV(MM) in order to understand its structural organization in relation to its biological function and its evolutionary relationship with other papovaviruses.

The genome of BKV has been extensively analyzed by physical mapping (*25*) with the use of 16 restriction enzymes. A detailed map including more than 100 sites on the genome has been constructed (*23, 26*). The BKV(MM) genome codes for four known BKV proteins (Fig. 1): T antigen, VP1, VP2, and VP3. The noncoding regions amount to about 12 percent of the genome. The general organization of the BKV(MM) genome is very similar to that of the more extensively studied SV40 (*27, 28*).

The complete nucleotide sequence of BKV(MM) DNA, which contains 4963 base pairs, is shown in Fig. 2. Regions coding for putative proteins are indicated in the right-hand margin. The early region codes for the T and t antigens. The late region codes for VP2, VP3, and VP1. The noncoding region includes the origin of DNA replication, repeated sequences, and palindromes, which may be involved in the regulation of transcription and translation.

Comparison of the genomes of BKV(MM) and BKV(WT) was made by detailed physical mapping and sequence analysis. Physical mapping revealed that the two genomes are essentially identical except in the regions shown in Fig. 3. The regions from map positions 0 to 0.512 and 0.699 to 1.0 on BKV(MM) are identical to those of 0 to 0.489 and 0.711 to 1.0, respectively, on BKV(WT). Differences between BKV(WT) and BKV(MM) are localized in the regions marked with stripes.

The sequence of BKV(WT) between map positions 0.520 to 0.712 is shown in Fig. 4. This sequence corresponds to the upper strand of the BKV(MM) between nucleotides 2701 to 3467 (Fig. 2). In this region, the sequence of BKV(WT) DNA is longer than that of BKV(MM) DNA by 233 nucleotide pairs. This difference is mainly accounted for by a 262-base deletion in BKV(MM) between nucleotides 2751 to 3014 of BKV(WT).

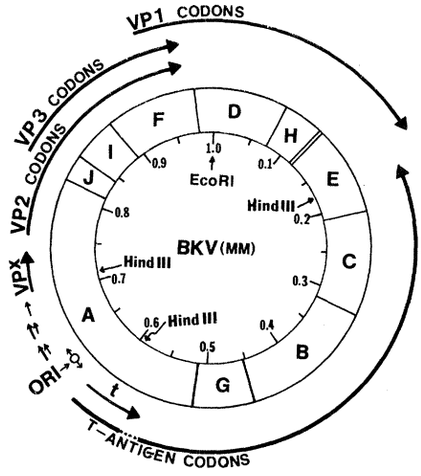

Fig. 1. Genetic organization of BKV DNA. The genome of BKV (strain MM) is presented as a circle. The unique *Eco* RI site is taken as 0 or 1.0 map position. The standard restriction cleavage map shown here to serve as physical reference consists of three *Hind* III sites in the inner circle and 11 *Mbo* I sites in the middle circle. The 11 *Mbo* I fragments thus generated are designated A to K (K, situated between H and E, is not shown). The major gene loci are indicated with arrows on the outer circle. Arrows start from the amino termini of the genes and the arrowheads represent the location of the carboxyl termini. The origin of DNA replication (Ori) is located at about map position 0.636. The nucleotide sequence (5′ → 3′) starting counterclockwise after Ori until map position 0.178 represents the early region which codes for T antigens. The sequence (5′ → 3′) clockwise from Ori to map position 0.163 represents the late region, which codes for several viral proteins including VP2, VP3, and VP1. The repeated small arrows located between Ori and VPx indicate tandem repeats of nucleotide sequences.

We have also determined the sequence of BKV(WT) DNA in several other regions, including map positions 0.15 to 0.21, 0.302 to 0.415, 0.450 to 0.520, and 0.712 to 0.750. No differences have been found between BKV(WT) and BKV(MM). However, minor differences in other regions of the two genomes cannot be ruled out.

The overall DNA sequence homology between BKV(WT) and SV40 DNA is 69 percent. The homology value starting from map positions 0 to 0.025 (2.5 percent of the genome) is 79 percent. The values of successive 0.025 map units are (percent): 76, 78, 79, 80, 78, *34*, *43*, *41*, 63, 72, 79, 78, 73, 75, 76, 73, 77, 76, 77, 71, 67, 68, 59, 73, 77, 54, *34*, *39*, 76, 64, 84, 79, 79, 69, 74, 58, 84, 84, 64. Thus, the value is from 64 to 84 percent in the majority of the regions, and from 34 to 43 percent homology between map positions 0.15 to 0.225 and 0.675 to 0.725. These values are somewhat lower than the 85 percent overall homology obtained by heteroduplex analysis (*19*). However, when a value of lowering the melting temperature (T_m) of 0.7°C (instead of 1.4°C) for every 1 percent mismatch in the DNA sequence (*29*) is used, the homology values from heteroduplex analysis (*19*) become very close to those obtained by sequence analysis.

BKV is closely related to SV40. Well-established facts about SV40 can be used as a guide to interpret DNA structure and function relationships of BKV. Cells infected or transformed by SV40 synthesize an early messenger RNA (mRNA). This mRNA is transcribed counterclockwise and hybridizes to the SV40 genome from map positions 0.65 to 0.17 (*13*). Since BKV complements the early mutant tsA58 of SV40 (*5*), and the sizes of BKV and SV40 T antigens are similar, it may be assumed that the early region of BKV(MM) also codes for a T antigen starting from 0.614 map position (Fig. 1) counterclockwise to 0.178. A potential initiation signal for translation is located between nucleotides 3047 and 3045 (lower strand) in Fig. 2. From this point on, there is only one open reading frame which can code for a polypeptide of 100 amino acids (*10, 24*). This polypeptide corresponds to the putative t antigen. By comparing this sequence with that of the SV40 t antigen, a striking similarity in amino acid sequence is evident. Among the first 74 amino acids from the amino terminus, 64 are identical. Ten additional amino acid residues are chemically similar [for example, Leu and Ile (leucine and isoleucine), Asp and Glu (aspartic acid and glutamic acid)]. The high degree of similarity leads us to conclude that the


Eco RI
MboI(1)
MboI(2)
MboI(3)
MboI(4)
MboI(5)
MboI(6)
MboI(7)
HindIII(1)
XbaI(1)
SacI(1)
PstI
VP1 CODONS
T2 ANTIGEN CODONS

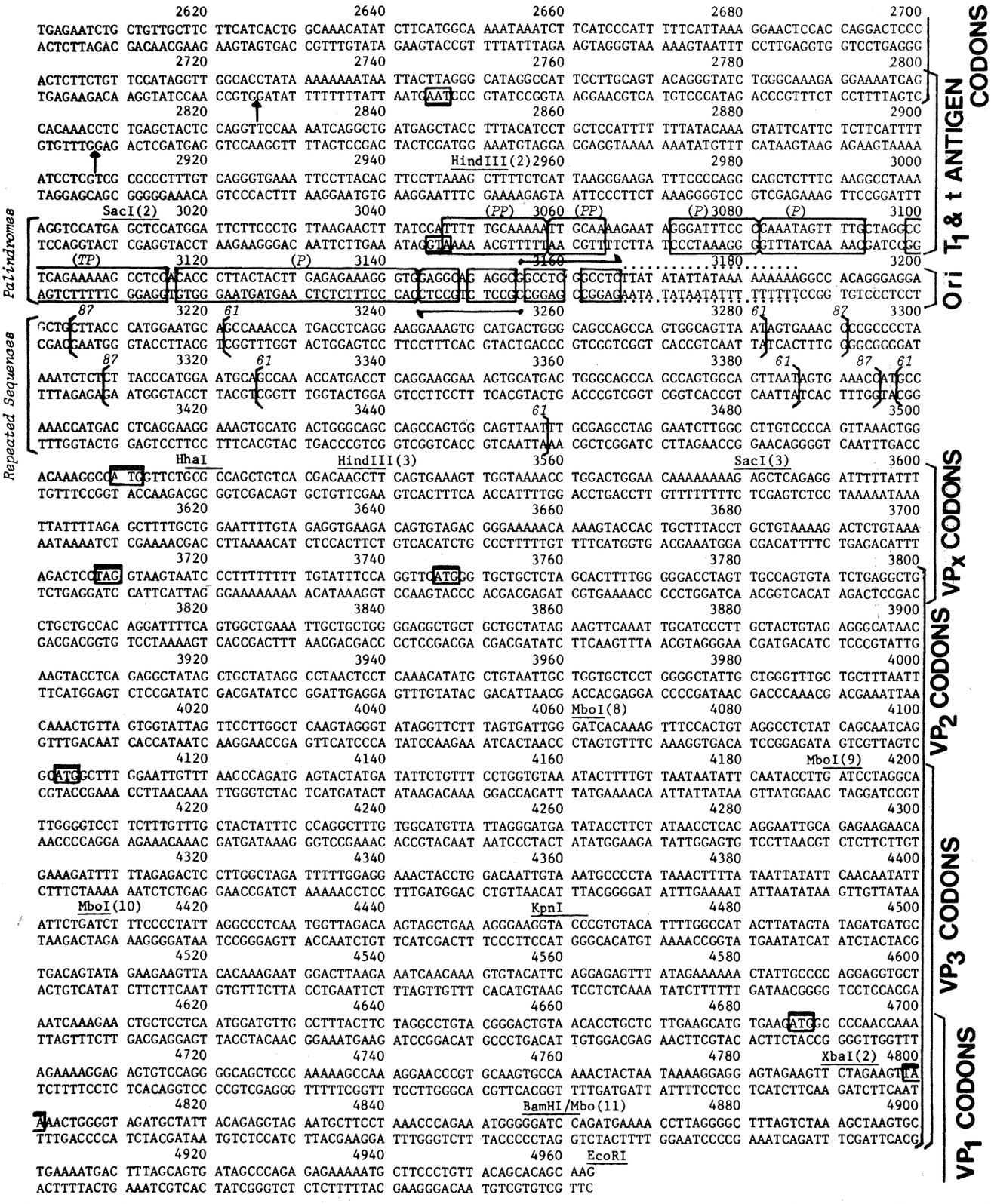

Fig. 2. Nucleotide sequence of BKV (strain MM) DNA. The DNA sequence was determined by the method of Maxam and Gilbert (*36*). The partial degradation products were analyzed by fractionation in 0.4-mm thick gels (*37*), 80 cm in length (*10*). Approximately 85 percent of the genome was sequenced from both strands, and the complete sequence of the DNA is given . The upper strand gives the 5′ to 3′ direction from left to right. The second base of the unique *Eco* RI hexanucleotide recognition sequence is taken as nucleotide 1. This is intended to coincide with the usage of the *Eco* RI site as 0 or 1.0 map position for the standard physical map shown in Fig. 1. The cleavage sites of *Hin*d III, *Mbo* I, *Xba* I, and *Sac* I are each given in consecutive numbers starting clockwise after the *Eco* RI site. The cleavage sites of single-cut enzymes, *Pst* I, *Hha* I, *Kpn* I, and *Bam* HI, are also indicated. Triplets corresponding to initiation and termination codons of each gene are boxed in. The location of each gene locus is given at the right-hand margin. That of palindromes (a double-stranded DNA sequence with a twofold rotational symmetry) and the tandemly repeated sequences is indicated at the left-hand side (P, palindrome; PP, perfect palindrome; and TP, true word palindrome). The origin of replication (Ori), also a palindrome, is boxed in with a pair of reverse arrows. Sets of repeated sequences are confined within pairs of brackets together with italic numbers indicating the length of each repeat. An A·T-rich region is marked with dotted lines. T_1 and T_2 stand for the first and second portion of the T antigen. This figure includes the partial sequences and correction of several errors reported earlier (*10, 29*).

region from map positions 0.614 to 0.554 on BKV(MM) codes for t antigen. In one respect the predicted BKV(MM) t antigen differs from that of SV40: it contains 100 amino acids as compared to the 174 of SV40. On the other hand, in BKV(WT) the putative t antigen is 172 amino acids in length (data not shown).

In SV40, the T antigen is coded for by two noncontiguous segments of DNA in the early region (*28, 30*). The first 82 amino acids in T antigen are identical to those in t antigen. The SV40 early mRNA is spliced to a point 347 nucleotides away and the mRNA from that point on codes for another 626 amino acids before reaching a termination codon at map position 0.172. At the junction of splicing, the sequence AGGU (A, adenine; G, guanine; U, uracil) appears. This sequence or a related sequence, such as CAGG (*31*) (C, cytosine), has been found at the junction of splicing of other eukaryotic mRNA's, and it may be a part of the sequence recognized by the splicing enzyme. Since a large number of AGGT (T, thymine) sequences occur in the SV40 and BKV genomes and only a few points are involved in RNA splicing, there must be additional sequences or secondary structural information (*32*) involved in providing the necessary specificity.

In BKV(MM) DNA, at a region corresponding to the SV40 T antigen coding sequence, an AGGT occurs between nucleotides 2809 and 2806 (lower strand). Thus, it is likely that the mRNA of T antigen is also spliced at this point and joined to nucleotide 2725 (within another AGGT sequence), the starting point for the remainder of the T antigen coding se-

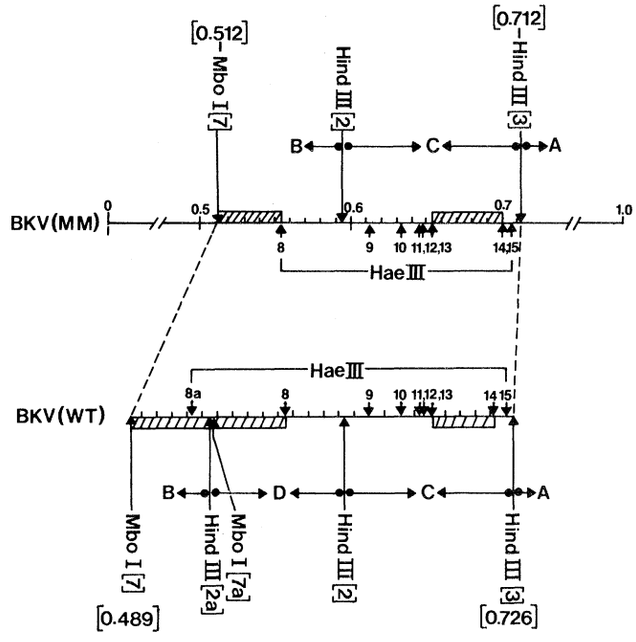

Fig. 3. Differences between the genomes of BKV (prototype, WT) and BKV (MM strain) as revealed by physical mapping. Extensive physical mapping by restriction enzymes of both BKV(MT) and BKV(MM) DNA has been carried out (*38*). The physical maps include map positions 0.512 to 0.712 for BKV(MM) DNA and 0.489 to 0.726 for BKV(WT) where differences between the two genomes lie. Cleavage sites of each restriction enzyme are consecutively numbered starting clockwise (from left to right) after the *Eco* R1 site. The shaded regions between cleavage sites 7 for *Mbo* I and 8 for *Hae* III as well as sites 13 and 14 for *Hae* III show differences in size of restriction fragments of the two genomes. The DNA sequence of this region is shown in Fig. 4.

```
ACTCTTCTGTTCCATAGGTTGGCACCTATAAAAAAAATAATTACTTAGGGCCTTTTAATATTTTATTATTTATCTAAATA 2780
TAAGTTAGTTACCTTAAAGCTTTAGATCTCTGAAGGGAGTTTCTCCAATTATTTGGACCCACCATTGCAGAGTTTCTTCA 2860
GTTAGGTCTAAGCCAAACCACTGTGTGAAGCAGTCAATGCAGTAGCAATCTATCCAAACCAAGGGCTCTTTTCTTAAAAA 2940
TTTTCTATTTAAATGCCTTAATCTAAGCTGACATAGCATGCAAGGGCAGTGCACAGAAGGCTTTTTGGAACAAATAGGCC 3020
ATTCCTTGCAGTACAGGGTATCTGGGCAAAGAGGAAAATCAGCACAAACCTCTGAGCTACTCCAGGTTCCAAAATCAGGC 3100
TGATGAGCTACCTTTACATCCTGCTCCATTTTTTTATACAAAGTATTCATTCTCTTCATTTTATCCTCGTCGCCCCCTTT 3180
GTCAGGGTGAAATTCCTTACACTTCCTTAAATAAGCTTTTCTCATTAAGGGAAGATTTCCCCAGGCAGCTCTTTCAAGGC 3260
CTAAAAGGTCCATGAGCTCCATGGATTCTTCCCTGTTAAGAACTTTATCCATTTTTGCAAAAATTGCAAAAGAATAGGGA 3340
TTTCCCCAAATAGTTTTGCTAGGCCTCAGAAAAAGCCTCCACACCCTTACTACTTGAGAGAAAGGGTGGAGGCAGAGGCG 3420
GCCTCGGCCTCTTATATATTATAAAAAAAAAGGCCACAGGGAGGAGCTGCTTACCCATGGAATGCAGCCAAACCATGACC 3500
TCAGGAAGGAAAGTGCATGACTCACAGGGGAATGCAGCCAAACCATGACCTCAGGAAGGAAAGTGCATGACTCACAGGGA 3580
GGAGCTGCTTACCCATGGAATGCAGCCAAACCATGACCTCAGGAAGGAAAGTGCATGACTGGGCAGCCAGCCAGTGGCAG 3660
TTAATAGTGAAACCCCGCCGACAGACATGTTTTGCGAGCC
```

Fig. 4. Nucleotide sequence of BKV(WT). The DNA sequence between map positions 0.520 to 0.712 on BKV(WT) is given. The DNA sequence presented here is between nucleotides 2701 to 3700, corresponding to map position 0.544 to 0.699 on BKV(MM) genome. The nucleotides that are underlined indicate homology with the BKV(MM) DNA sequence. The nonhomologous parts are due to addition, deletion, or base changes when compared to BKV(MM) DNA.

quence. The predicted amino acid sequence of the second portion of the BKV(MM) T antigen contains 614 amino acids. Within the first 525 amino acids it shows 80 percent homology with the SV40 T antigen.

As in SV40, there is insufficient coding capacity for the BKV(MM) T antigen unless another segment of mRNA is spliced onto the mRNA which codes for the major part of the T antigen (map positions 0.55 and 0.17). Thus, the BKV(MM) T antigen is probably also coded for by two noncontiguous segments of DNA.

In both BKV(MM) and SV40, the nucleotide sequences at the 5′ noncoding region of the T antigen genes also show remarkable homology. Immediately before the AUG initiation codon a stable secondary structure may form. It contains an 8-base pair double-stranded stem adjacent to a hairpin loop (*24*). This potential secondary structure may be involved in regulating transcription or translation of the T antigen mRNA.

The late coding region starts at map position 0.707 (Fig. 1) and extends clockwise to map position 0.163 (nucleotide 808). There is a potential initiation codon ATG at positions 3510 to 3512. Starting from this reading frame, the DNA sequence can code for a putative protein of 66 amino acids in length, designated VPx, which has not yet been isolated from this or related viruses. The corresponding region of the SV40 genome can code for a similar protein of 62 amino acids with 40 amino acids being identical to those of BKV(MM). It has been reported that an abundant RNA species of SV40 is complementary to the DNA sequence in this region (*28*).

Starting from the ATG coding sequence at 3746 to 3748 (Fig. 2), the sequence of a protein of 351 amino acids in length (data not shown) can be deduced from the only reading frame. Within the first 41 amino acids of this protein, 38 are identical to those of VP2 of SV40. The overall amino acid homology between the putative VP2 of BKV(MM) and that of SV40 is 77 percent. This very high degree of homology is not likely to occur by chance, and thus this region of the BKV(MM) genome most likely codes for VP2. The amino acid composition of VP2 is rather unusual. The region within the first 99 amino acids from the amino terminus is very rich in hydrophobic amino acids, and there are no basic amino acids. The central region of VP2, between amino acids 121 to 220, is devoid of methionine, cysteine, and lysine. Finally, among the 33 amino acids at the carboxyl terminus, 14 are basic amino acids; there are no acidic amino acids.

The initiation codon for VP3 is located at nucleotides 4103 to 4105, within the VP2 gene. The amino acid sequence of VP3 is a subset of VP2 and shares amino acids 120 to 351.

The gene coding for VP1 protein starts at nucleotide 4686. A protein 362 amino acids in length (data not shown) can be deduced from a unique reading frame of the DNA sequence. There is an overall 79 percent amino acid homology with SV40 VP1. The VP1 coding sequence initiates at a point 113 nucleotides within the gene coding for the carboxyl terminus of VP2 and VP3, but uses a different reading frame. Thus, this region of the BKV(MM) genome codes for three different proteins in two different reading frames. Overlapping genes have also been reported for SV40, where the VP1 gene overlaps 110 nucleotides with the VP2/VP3 gene (*27, 28*), and for bacteriophage ϕX174 (*33*). The overlapping of genes is expected to restrict the accumulation of mutations since each mutation may affect the sequence of three polypeptides. However, a comparison of the BKV and SV40 sequences does not support this expectation. Changes in the nucleotide sequence coding for VP1 or VP2/VP3 as well as changes in the amino acid sequence of these proteins appear to be as frequent as those of nonoverlapping genes.

Certain DNA sequences are directly repeated on the genome of BKV(MM). The repeated sequences and palindromic sequences are mainly located at map positions 0.614 to 0.707 on BKV(MM), a region which does not code for any known protein. This region includes the origin of DNA replication and the sites at which the transcription of early and late mRNA are initiated in SV40 and probably in BKV (*21, 27, 28*). Within this region SV40 T antigen also binds (*34*) and exerts a regulatory function on DNA synthesis. Presumably, the same is also true of BKV T antigen.

As shown in Figure 2, there are several palindromes in the noncoding region. The origin of DNA replication (Ori) is characterized by G-C rich inverted repeats of G-C-C-T-C, which can be drawn as long hairpin loops. These G-C rich palindromes are also found near or at the origin of replication of SV40 (*27, 28*), polyoma virus (*35*), and wild-type BKV (*21*). There are several direct repeats within this region (shown between brackets in Fig. 2). In BKV(MM), there are two 87 nucleotide-long segments and three 61 nucleotide-long segments (two of which are a part of the 87-long repeats). These include three 36-base repeats identical to those in BKV(WT). Repeated sequences have also been reported in SV40 (*27, 28*); however, the sequences as well as the pattern of these repeats are different from those of BKV. These repeated sequences may come from the host cells by recombination.

ROBERT C. A. YANG
RAY WU
Section of Biochemistry, Molecular and Cell Biology, Cornell University, Ithaca, New York 14853

References and Notes

1. S. D. Gardner, A. M. Field, D. V. Coleman, B. Hulme, *Lancet* **1971-I**, 1253 (1971).
2. K. K. Takemoto, A. S. Rabson, M. F. Mullarkey, R. M. Blaese, C. F. Garon, D. Nelson, *J. Natl. Cancer Inst.* **53**, 1205 (1974).
3. R. A. Gatti and R. A. Good, *Cancer* **28**, 89 (1971).
4. J. Seehafer, A. Salmi, D. G. Scraba, J. S. Colter, *Virology* **66**, 192 (1975).
5. D. A. Mason and K. K. Takemoto, *J. Virol.* **17**, 1060 (1976).
6. S. D. Gardner, *Br. Med. J.* **1973-I**, 77 (1973).
7. K. V. Shah, R. N. Daniel, S.Worzawski, *J. Infect. Dis.* **128**, 784 (1973); K. V. Shah, R. N. Daniel, J. D. Strandberg, *J. Natl. Cancer Inst.* **54**, 965 (1975).
8. K. K. Takemoto and M. F. Mullarkey, *J. Virol.* **12**, 625 (1973).
9. P. M. Howley, G. Khoury, J. C. Bryne, K. K. Takemoto, M. A. Martin, *Virology* **16**, 959 (1975).
10. R. C. A. Yang and R. Wu, *Proc. Natl. Acad. Sci. U.S.A.* **76**, 1179 (1979).
11. E. O. Major and G. di Mayorca, *ibid.* **70**, 3210 (1973); J. Van der Noordaa, *J. Gen. Virol.* **30**, 371 (1976).
12. M. Portolani, G. Barbanti-Brodano, M. LaPlaca, *J. Virol.* **15**, 420 (1975).
13. T. K. Kelly and D. Nathans, *Adv. Virus Res.* **21**, 85 (1977); G. C. Fareed and D. Davoli, *Annu. Rev. Biochem.* **46**, 471 (1977).
14. B. E. Griffin and M. Fried, *Methods Cancer Res.* **12**, 49 (1976).
15. D. T. Simmons, K. K. Takemoto, M. A. Martin, *J. Virol.* **24**, 319 (1977).
16. M. F. Mullarkey, J. F. Hruska, K. K. Takemoto, *ibid.* **13**, 1014 (1974); P. J. Wright and G. di Mayorca, *ibid.* **15**, 828 (1975); G. Barbanti-Brodano, G. P. Minelli, M. Portolani, L. Lambertini, M. Toppini, *Virology* **64**, 269 (1975).
17. G. Khoury, P. M. Howley, C. Garon, M. F. Mullarkey, K. K. Takemoto, M. A. Martin, *Proc. Natl. Acad. Sci. U.S.A.* **72**, 2563 (1975); W. S. M. Wold, J. K. Mackey, K. H. Brackmann, N. Takemori, P. Rigden, M. Green, *ibid.* **75**, 454 (1978).
18. J. E. Osborn, S. M. Robertson, B. L. Pagett, D. L. Walker, B. Weisblum, *J. Virol.* **19**, 675 (1976).
19. N. Newell, C.-J. Lai, G. Khoury, T. J. Kelly, Jr., *ibid.* **25**, 193 (1978).
20. P. M. Howley, M. A. Israel, M. F. Law, M. A. Martin, *J. Biol. Chem.* **254**, 4876 (1979).
21. R. Dhar, C. Lai, G. Khoury, *Cell* **13**, 345 (1978).
22. R. Dhar, I. Seif, G. Khoury, *Proc. Natl. Acad. Sci. U.S.A.* **76**, 565 (1979).
23. R. C. A. Yang and R. Wu, *ibid.* **75**, 2150 (1978).
24. ———, *Virology* **92**, 340 (1979).
25. K. J. Danna and D. Nathans, *Proc. Natl. Acad. Sci. U.S.A.* **68**, 2913 (1971); K. J. Danna, G. H. Sack, D. Nathans, *J. Mol. Biol.* **78**, 363 (1973); H. O. Smith and M. L. Birnstiel, *Nucleic Acids Res.* **3**, 2387 (1976); E. Jay and R. Wu, *Biochemistry* **15**, 3612 (1976).
26. R. C. A. Yang and R. Wu, *J. Virol.* **27**, 700 (1978); *ibid.* **28**, 851 (1978); J. Freund, G. di Mayorca, K. N. Subramanian, *ibid.* **29**, 915 (1979).
27. W. Fiers, R. Contreras, G. Haegeman, R. Rogiers, A. Van de Voorde, H. Van Heuverswyn, J. Van Herreweghe, G. Volckaert, M. Ysebaert, *Nature (London)* **273**, 113 (1978); and some references cited therein.
28. V. B. Reddy, B. Thimmappaya, R. Dhar, K. N. Subramanian, B. S. Zain, J. Pan, P. K. Ghosh, M. L. Celma, S. M. Weissman, *Science* **200**, 494 (1978); and references cited therein.
29. C. D. Laird, B. L. McConaughy, B. J. McCarthy, *Nature (London)* **224**, 149 (1969).
30. P. K. Ghosh, V. B. Reddy, J. Swinscoe, P. V. Choudary, P. Lebowitz, S. M. Weissman, *J. Biol. Chem.* **253**, 3643 (1978); A. J. Berk and P. A. Sharp, *Proc. Natl. Acad. Sci. U.S.A.* **75**,

1274 (19′ → Y. Aloni, R. Dhar, O. Laub, M. Horowitz, G. Khoury, *ibid.* **74**, 3686 (1977).
→ R. Breathnach, B. Benoist, K. O'Hare, F. Gannon, P. Chambon, *ibid.* **75**, 4853 (1978).
32. M. Philipp, D. Ballinger, H. Seliger, *Naturwissenschaften* **65**, S-338 (1978).
33. F. Sanger, G. M. Air, B. G. Barrell, N. L. Brown, A. R. Coulson, J. C. Fiddes, C. A. Hutchison, III, P. M. Slocombe, M. Smith, *Nature (London)* **265**, 687 (1977).
34. R. Tjian, *Cell* **13**, 165 (1978).
35. E. Soeda, G. Kimura, K. Miura, *Proc. Natl. Acad. Sci. U.S.A.* **75**, 162 (1978); T. Friedmann, P. LaPorte, A. Esty, *J. Biol. Chem.* **253**, 6561 (1978); E. Soeda, J. R. Arrand, N. Sinolar, B. E. Griffin, *Cell* **17**, 357 (1979).
36. A. M. Maxam and W. Gilbert, *Proc. Natl. Acad. Sci. U.S.A.* **74**, 560 (1977).
37. F. Sanger and A. R. Coulson, *FEBS Lett.* **87**, 107 (1978).
38. R. C. A. Yang and R. Wu, in preparation.
39. Supported by National Institutes of Health grant CA-14989, and American Chemical Society grant VC-216.

12 June 1979; revised 27 August 1979

Bird Predation on Forest Insects: An Exclosure Experiment

Abstract. *Exclusion experiments show that birds significantly reduce densities of larval Lepidoptera on forest understory vegetation. When insect densities are already low, bird predation may act both as a population regulator and as a strong agent of natural selection.*

Insectivorous birds can be expected to influence their prey populations in at least two major ways. First, they may act as regulators of insect abundance, an effect that has been the subject of lengthy debate, especially as it applies to herbivorous insects (*1*). Second, as visually hunting predators, they may exert strong selective pressures that result in the evolution of crypsis or other predator-avoidance adaptations among their insect prey (*2*). Few data, however, exist on the actual impact of birds on their prey in nature (*3*). We report experimental evidence that birds depress the abundance of free-living defoliating insects in a temperate deciduous forest.

In 1978, we measured the impact of bird predation in the summer on endemic levels of foliage-dwelling arthropods in a northern hardwood forest (*4*). We used crop protection netting (*5*) to exclude birds from patches of striped maple (*Acer pensylvanicum* L.), an understory shrub (*6*). Ten exclosures, measuring about 6 by 6 by 2 m high, were established in early June after leaf flush was complete. An area of approximately equal size, similar plant species composition, and foliage density was chosen near each exclosure to serve as a control. At weekly intervals from 15 June through 10 August, we selected 400 striped maple leaves within each exclosure and each control area, and visually made a census of all insects present on the leaves and adjacent petioles and stems (*7*).

The results differed among the arthropod groups. For Arachnida, Coleoptera, Homoptera, and Hemiptera, we observed no significant differences in densities between the control and the experimental groups in any single sampling period, or for the season as a whole (Table 1). Indeed, in some sampling periods, there were slightly more individuals outside than inside the netting. Although birds in this forest do prey on these arthropods (*8*), their effect was either negligible or unmeasurable in this experiment

Table 1. Densities of the major arthropod taxa on leaves of striped maple inside and outside of exclosures. Numbers per 400 leaves (mean ± 95 percent confidence limits) were based on samples taken from ten exclosures and ten controls at eight weekly intervals during the period 15 June through 10 August 1978.

Taxa	Exclosures	Controls	*P*
Arachnida	5.3 ± .88	5.5 ± .92	.84
Coleoptera	1.7 ± .37	2.2 ± .48	.08
Homoptera	1.4 ± .53	1.3 ± .31	.86
Hemiptera	2.3 ± .74	1.9 ± .46	.95
Lepidoptera larvae	3.3 ± .53	2.3 ± .44	.003

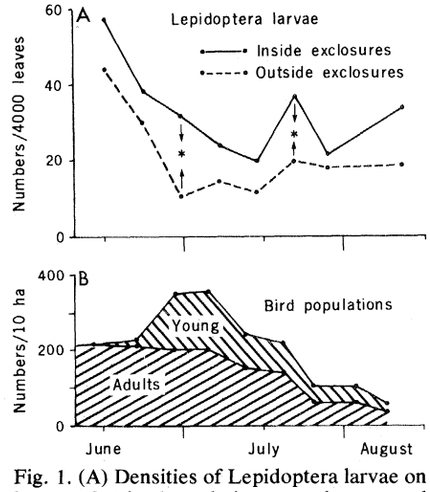

Fig. 1. (A) Densities of Lepidoptera larvae on leaves of striped maple in ten exclosures and in ten outside control plots (asterisks indicate $P < .05$). (B) Densities of adult birds and of their fledged young in the Hubbard Brook Experimental Forest (*12*).

because of the relatively high mobility of these kinds of prey.

The numbers of the more sedentary Lepidoptera larvae (*9*), however, were always higher inside the exclosures than outside (Fig. 1A). Because variances in the density data approximated the means, large differences were needed for statistical significance (*10*). When the numbers of Lepidoptera larvae are considered for the season as a whole (Table 1), significantly fewer Lepidoptera ($P < .003$) were found outside than inside the exclosures. In addition, we could distinguish statistically significant differences in the abundances of Lepidoptera larvae on two sampling dates, 29 June ($P < .02$) and 21 July ($P < .05$).

Since birds are the only element in the system excluded by the netting (*11*), we estimate from Fig. 1A that the weekly removal rates of caterpillars from understory foliage by birds range from 18 to 63 percent, averaging 37 percent. This effect is most extreme in late June and mid-July (Fig. 1A), coinciding with the nestling and fledging periods of insectivorous birds in this forest (*12*). During this part of the summer the numbers and biomass of birds hunting or needing to be fed nearly doubles (Fig. 1B), and their predation intensity must increase accordingly. The birds primarily responsible for this predation in the understory at Hubbard Brook were two warblers (*Seiurus aurocapillus* and especially *Dendroica caerulescens*), two thrushes (*Catharus ustulatus* and *C. fuscescens*), and several species that expand their vertical foraging ranges into the understory during the nestling and early fledgling periods (*Vireo olivaceus, V. philadelphicus*, and *Setophaga ruticilla*). That Lepidoptera larvae are a major food for most passerine birds, especially when young are being fed (*8, 13*) explains why the more significant depression of caterpillar numbers occurs at this time.

The proportion of the caterpillar standing crop removed in our experiment greatly exceeds the 0.1 to 1 percent reportedly taken by birds during most caterpillar outbreaks (*14, 15*). This suggests that, although birds seem to be unimportant as control agents during insect epidemics, they can depress further the numbers of caterpillars when the latter are already at low densities. Our results therefore provide experimental evidence supporting the suppositions of Tinbergen (*16*), Morris *et al.* (*15*) and Campbell and Sloan (*17*) that bird predation may be most effective at endemic prey population levels. The effect at these times is to reduce insect numbers at least locally

0036-8075/79/1026-0462$00.50/0